Synthesis of 4-Chloro-1,3-Diazobenzene Bent-Cores Liquid Crystal and Characterisations of Its Mesogenic Behaviour and Photosensitivity

Jinying Lu[a], Zelong Zhang[b*], Daoren Yan[a], Zhiyong Zhang[a]*, Jintao Guan[a], and Junfei Qiao[a]

[a]Department of Chemistry and Environmental Engineering, Wuhan Polytechnic University, Wuhan, China; [b]Department of Geology and Geophysics, Louisiana State University, Baton Rouge, LA, USA

Corresponding authors*

Dr. Zelong Zhang zelongz@lsu.edu

Prof. Zhiyong Zhang zzy6211@126.com

Abstract

Azobenzene-based bent-core liquid crystals demonstrate a variety of mesomorphic behaviours and photochromic properties which are desirable for optical switching. In this study, a novel compound **4c** was synthesised by adding azo functional groups and chlorine substituent to the central bent-core. The structure, mesogenic properties, and photosensitivity of **4c** was characterised by fourier-transform infrared spectroscopy (FTIR), ^{1}H and ^{13}C nuclear magnetic resonance (NMR), mass spectrometry (MS), differential scanning calorimetry (DSC), polarised optical microscopy (POM), and ultraviolet–visible spectroscopy (UV-Vis). The experimental results show that **4c** exhibited a broad temperature window of nematic phase (63.8 °C), rapid *trans* – *cis* photoisomerisation in seconds, and high *cis* fraction of 0.81. At room temperature, **4c** dissolved in ethyl acetate can reach photostationary state in 10 seconds. At 95 °C, nematic **4c** became isotropic under UV irradiation in 3 seconds and can be restored to be nematic under natural visible light in 5 seconds. Quantum mechanics calculations confirm that using azos instead of esters as the central linkages can effectively reduce the molecular dipole moment and enhance the overall molecular polarisabilities, which promotes favourable mesogenic and photonic behaviours. This study provides novel synthesis route and synergistic approach to advance the design of azobenzene bent-core liquid crystals.

Keywords:

bent-core liquid crystal; 4-chloro-1,3-diazobenzene; synthesis; nematic phase; photoisomerisation; quantum mechanics calculation;

1. Introduction

Photosensitive liquid crystals, especially azobenzene-based bent-core liquid crystals

(ABLCs), are promising materials for optical switching.[1–4] ABLC compounds can be highly photochromic and mesogenic due to the reversible *trans-cis* photoisomerisation of azo group (–N=N–) induced by proper irradiation of ultraviolet or visible light.[5,6] These characteristics also give rise to a myriad of potential applications of ABLC in areas such as elastomer, holographic imaging, optical data storage, and nanomachines.[7–11]

To date, the majority of ABLC compounds implemented at least one ester as the direct linkage of the central bent-core and or deployed azo groups in the distant side arms,[5,12–17] which usually exhibited high temperatures of phase transition, far above room temperature 25 °C, and narrow temperature ranges of nematic phases. To lower the phase transition temperature and broaden the temperature range of nematic phases, recent studies emphasised on structural alterations such as introducing different lateral substitutions on the bending core, [12,13,18] adjusting the number of aromatic units,[14,19–21] modifying the type, number, and position of linkage groups,[14,22–25] and changing the type and length of the terminal chains.[14,15,25–27] Yet, the mesogenic phase behaviours of current ABLCs are still unfavourable for practical applications.

We hypothesised that the linking groups adjacent to the central bent-core play a vital role in determining the mesogenic properties of ABLCs. The ester groups commonly used on the central bent-cores as the linking units can induce strong electrostatic forces that contribute to the intermolecular interactions of ABLCs, leading to high phase transition temperatures and narrow nematic phases. Previous studies suggest that the location of azo linkage does not exert significant influence on the mesogenic behaviour; if azo bond is close to central ring, it can even inhibit the formation of mesogenic phases.[14,22] However, their conclusions were based on compounds with a single azo linkage. This study proposed an alternative approach to improve the design of ABLC by using two azo bonds instead of esters as the central linkages connecting the central bent-core,

which intends to weaken the intermolecular interactions and therefore to enhance the overall performance of ABLC. ABLC compound synthesised in this study was derived from 4-chloro-1,3-diazobenzene. It has two azo linkages and one chlorine substituent in the 1,3-position and 4-position, respectively, at the central aromatic ring and terminal alkyl chains.

2. Materials and methods

2.1 Materials

Anhydrous aluminum trichloride (chemically pure), N, N'-dicyclohexylcarbodiimide (DCC), and 4-dimethylaminopyridine (DMAP) were obtained from Tianjin Fuchen Chemical Reagent (China), Nanjing Chemical Reagent (China), and Xiya Reagent (China), respectively. All chemicals used in this study are of analytical grade, unless otherwise stated. 4-n-hexylbenzoic acid, 4-n-heptylbenzoic acid, 4-n-octylbenzoic acid, 4-n-decylbenzoic acid, and 4-n-decylbenzoic acid were synthesised in our laboratory. Reaction products were purified by silica gel column chromatography and recrystallised three times from ethanol – dichloromethane 1:1 mixture.

2.2 Characterisation

Reactions required low temperature were conducted in Zhengzhou Greatwall DHJF-8002 low temperature constant temperature stirring reaction bath. Infrared spectroscopy was performed by a Thermo Nicolet Avatar 330 FTIR. ^{1}H NMR spectra were obtained from a Varian INOVA 400 spectrometer (400 MHz) using tetramethylsilane (TMS) as the reference standard. Differential scanning calorimetry (DSC) experiments were conducted on a TA Instruments DSC Q-20 with a scanning rate of 5 °C/ min and natural cooling. Phase transition and optical textures of liquid crystal compounds were characterised by a polarising optical microscope (POM) XPN-100E from Shanghai Changfang Optical Instrument.

UV-Visible absorption spectroscopy was collected by a UV-8000S spectrophotometer from Shanghai Metash Instrument. UV-Vis experiments were conducted using a wavelength range from 200 nm to 550 nm and a scan rate of 1 nm/s. UV-Vis spectral data were used i. to measure the isomer fraction by dissolving sample in dilute solution of ethyl acetate (2.5×10^{-5} mol/L) at room temperature and ii. to characterise the UV-induced photoisomerisation of mesogenic phases at 95 – 100 °C. The data collection of UV-Vis spectroscopy was started when the absorbance value of the two consecutive measurements were identical.

2.3 Synthesis

Target compounds **4c** was synthesised according to Figure 1, of which the steps are described below.

2.3.1 Synthesis of 4-chloro-1,3-dinitrobenzene **(I)**[28]

Chlorobenzene (40 ml) was added in a 500 ml three-neck flask with magnetic stir bar. The temperature was maintained at 95 °C. Concentrated nitric acid (117.6 ml) and concentrated sulfuric acid (123.6 ml) were added in the flask. The solution mixture was stirred for 5 hours, in which the reaction was monitored by thin layer chromatography (TLC). The reaction product was washed with hot water to reach pH neutral, vacuum-filtered, and air-dried. This step produced yellow crystals.

Yield: 55.07 g, 85.2%, melting point (m.p.) 48 °C. FTIR (KBr, ν_{max}, cm^{-1}): 3082.32 (Ar–H), 1618.15, 1528.35 (Ar), 1474.40, 1352.32, 1306.78, 1202.84, 1102.45.

2.3.2. Synthesis of 4-chlorom-1,3-diaminobenzene **(II)**[29]

pure iron powder (28 g, 0.5 mol), glacial acetic acid (45 g), and 100 mL deionised water were added in a 250 mL three-necked flask. Once the solution was heated to 70 ~ 80 °C, compound

(**I**) (20.2 g, 0.1 mol) was added. The reaction was carried out for 4h, which was monitored by TLC to ensure the completion. The product mixture was filtered and washed with hot water two times to remove the nonpolar impurities. The pH of the filtrate was adjusted to pH 10.0 with saturated Na_2CO_3 solution. The organic phase was extracted with 30 mL ethyl acetate repeated for three times and then was dried with anhydrous K_2CO_3, yielding a crude black product. The product was purified by silica gel column chromatography. This step produced a needle-shaped brown solid of compound (**II)**.

Yield: 10.5 g, 74.2%, m.p. 86-88 °C. FTIR (KBr, ν_{max}, cm^{-1}): 3343.37, 3405.11, 3315.06 (N–H), 3211.17 (Ar–H), 1615.53, 1577.97, 1496.67, 1451.98 (Ar), 1333.37, 1274.30, 1208.48, 1147.56, 1106.67, 1044.15, 845.96.

2.3.3 Synthesis of 4-chloro-1,3-bis (4-hydroxyphenyl)azobenzene **(III)**[30]

Chilled concentrated hydrochloric acid (40 mL, 0.5mol) was added in a three-necked flask. The temperature was maintained below –25 °C. A solution prepared from sodium nitrite (12.5 g, 0.18 mol) and 19 mL deionised water was added dropwise while stirring slowly. Then, a solution prepared from compound (**II)** (7.15g, 0.05mol) and concentrated hydrochloric acid (25mL) was added in multiple steps while gradually increasing the stirring speed. The reaction was lasted for 0.5 hour, generating a yellow transparent liquid. Urea pellets (4.8 g, 0.08mol) were added into the liquid dropwise while stirring to yield a diazonium salt.

The diazonium salt was added slowly to a three-necked flask containing a solution of phenol (11.3g, 0.12mol), sodium carbonate (31.8g, 0.3mol) and water (200ml). The mixture in the flask was stirred for 3h in a cold-water bath, of which the reaction was monitored by the TLC. Once the reaction was completed, the mixture was filtered. The resultant filter cake was

recrystallised from ethanol. 10.96g of yellow crystals of compound (**III**) was obtained. Yield: 62.3%. m.p. 164 ~ 166 °C. FTIR (KBr, ν_{max}, cm^{-1}): 3333.1 (–OH), 1702.11, 1583.27, 1502.13, 1473.53 (Ar), 1256.44, 1223.10, 1192.22, 1069.13, 1028.42, 853.33; ^{1}H NMR (400 MHz, $CDCl_3$, δ, ppm): 8.31 (s, 1H), 7.95 ~ 7.97 (d, J = 8 Hz, 1H), 7.67 ~ 7.77 (m, 5H), 7.18 ~ 7.21 (t, J = 6 Hz, 4H), 5.08 (s, 2H); ^{13}C NMR (100 MHz, $CDCl_3$): 161.118, 152.732, 149.855, 130.145, 129.282, 124.259, 120.387, 118.365, 115.927. MS m/z (%): 353.65 (65.5, M+1), 231.67 (19.5), 111.67 (13.1).

2.3.4 Synthesis of ABLC compound **4c**[31]

Compound (**II**) (1.66 g, 5mmol), 4-alkylbenzoic acid (10mmol), DCC (12 mmol), DMAP (1.2 mmol) and CH_2Cl_2 (50mL) were added in a 100 mL three-necked flask. The mixture was stirred at room temperature for 24 hours, in which this reaction was monitored by TLC. Upon the completion of the reaction, the mixture was filtered and washed with CH_2Cl_2. The solute was extracted by evaporating the solvent under reduced pressure and then purified by silica gel column chromatography.

4-Chloro-1,3-bis(4-((4-heptylphenyl)acyloxy)-1-(E)-azophenyl)benzene **4c**: 2.48g yellow needle crystal, yield: 71.5%, m.p. 84 ~ 85.5 °C. FTIR (KBr, ν_{max}, cm^{-1}): 2918.17, 2849.16 (–CH2), 1169.63, 1645.76, 1613.79, 1542.68, 1507.81, 1450.59 (Ar), 1355.50, 1339.12, 1296.69, 1233.43, 1125.32, 841.01. ^{1}H NMR (400 MHz, $CDCl_3$) δ (ppm): 8.32 (s, 1H), 8.09 ~ 8.11 (d, J = 6.5 Hz, 4H), 7.99 ~ 8.01 (d, J = 8 Hz, 4H), 7.53 ~ 7.55 (t, J = 6.5 Hz, 1H), 7.18 ~ 7.20 (d, J = 8 Hz, 4H), 7.07 ~ 7.09 (d, J = 6.0 Hz, 4H), 2.60 ~ 2.63 (t, J = 6 Hz, 4H), 1.63 ~ 1.66 (m, 4H), 1.31 ~ 1.36 (m, 16H), 0.89 ~ 0.92 (t, J = 6 Hz, 6H). ^{13}C NMR (100 MHz, $CDCl_3$) δ (ppm): 164.819, 152.378, 152.352, 150.212,149.701, 130.321, 129.732, 128.715, 126.590, 125.356, 124.289, 122.425, 116.423, 36.222, 31.852, 31.225, 30.285, 29.285, 22.589, 14.152. MS m/z (%): 757.59 (71.10，

M+1), 587.70 (16.5), 295.58 (28.1).

2.3.4 Computational Simulations

To validate the hypothesis based on experimental data, computational simulations were performed to study the molecular geometry and molecular dipole moments at the ground states. Compound **4c** contains 104 atoms and 10 rotatable bonds, which generates approximate 60,000 conformers. Apparently, searching conformers of global energy minimum is not viable for computationally demanding simulations especially for those based on quantum mechanics. Therefore, this study first applied molecular mechanics methods to search conformers of global energy minimum. After the screening, molecular properties of the selected conformers were calculated by quantum mechanics techniques.

Initial geometry optimization and conformer search were based on molecular dynamics simulations, which were conducted by Avogadro 1.2.0, a free cross-platform programme. General Amber force field was used due to its specific parameterisation for organic molecules.[32–35] Geometry optimization was performed using steepest descent algorithm with a convergence energy of 10^{-7} kcal/mol. Input structural parameters of azobenzene moiety were adopted from previous density functional theory calculation and X-ray diffraction data.[36,37] To find the candidate conformers of the global energy minimum, systematic rotor search was carried out.

Final geometry optimizations were performed by MOPAC (Molecular Orbital PACkage, 2016 version), a general-purpose semi-empirical molecular orbital package free for academic and not-for-profit use, using PM7 Hamiltonian and Baker's EigenFollowing method.[38,39] To obtain molecular properties such as molecular dipole moment, density functional theory (DFT) calculations were computed through GAMESS (General Atomic and Molecular Electronic

Structure System, US), a general ab-initio quantum chemistry package,[40,41] of which the site licence is free for both academic and industrial users. Specifically, all DFT calculations applied restricted orbitals, 6-31G* basis set,[42,43] and B3LYP functional.[44,45] SCF convergence criteria is set to 10^{-5} of the density matrix. Molecular dipole moments were obtained by single-point energy calculations. Time-dependent density functional theory computations were carried out to simulate the excited states for UV-Vis, of which the spectra were convoluted using Gaussian profiles provided by cclib library.[46] The simulated UV-Vis spectra are comparable to the experimental results as shown in Figure S1, which confirms that the *trans* and *cis* configurations of **4c** are reasonably represented in our study. Static polarisability and dynamic polarisabilities were obtained to elucidate photonic behaviours,[47] which were calculated by MOPAC using PM7 Hamiltonian.[48] Specifically, static polarisability was measured based on the response of the heat of formation and the dipole to an applied uniform electric field. Polarisabilities calculated from the response of both attributes were consistent given that the numerical difference is within 0.2%. Frequency-dependent dynamic polarisabilities were calculated by time-dependent Hartree-Fock theory, yielding first, second, and third-order polarisabilities.[48] Due to the complexity to express polarisabilities, here we only compare measurements at zero frequency including the isotropic average of first-order polarisabilities (α) and compare the average second harmonic generation (SHG) of the second-order polarisabilities (β) and the mean value of third polarisability (γ). A detailed list of polarisability values at different frequencies is summarised in Table S1. Notably, the isotropic averages of first-order polarisabilities (α) at zero frequency are identical to the average values of static polarisability, as posited by the theory.[47]

3. Results and discussion

In this study, an ABLC compound **4c** comprises a 4-Cl-1,3-m-phenylene rings as the central

bent cores, two azo bonds as the linkages of the central core, two ester groups as lateral arm bridges, and linear alkyl groups as the terminal chains, as shown in Figure 1 and Figure 5. This compound was characterised by FTIR, ^{1}H NMR, ^{13}C NMR, and mass spectrometry. Its mesogenic properties were examined by DSC and POM. Photoisomerisation phenomena were characterised by UV-Vis spectroscopy. The experimental results show that (1) the structure of compound **4c** is consistent with our design and (2) **4c** exhibited low melting point and wide temperature window of nematic phase. The effects of azo groups on the phase behaviours are also discussed.

3.1 Phases transition temperatures and enthalpies of compounds 4c

DSC analysis in Figure 2 shows that while increasing temperature compound **4c** displayed the following phases: crystalline solid (Cr), smectic (Sm), nematic (N), and isotropic liquid (Iso). The temperatures of phase transitions are 84.52 °C for Cr – Sm, 91.36 °C for Sm – N, and 155.20 °C for N – Iso. Additionally, the enthalpies for Cr – Sm, Sm – N, and N – Iso transitions are 33.7 kJ/mol, 7.4 kJ/mol, and 2.95 kJ/mol, respectively. Notably, **4c** displayed a wide temperature window 70.68 °C for mesogenic phase and 63.84 °C for nematic phase. The polarised micrograms of different phases of **4c** on heating are listed in Figure 3. Specifically, **4c** displayed i. a typical columnar texture in smectic phase at 88 °C (Figure 3.1), ii. a schlieren texture in nematic phase at 120 °C (Figure 3.2), and iii. isotropic liquid phase at 155 °C (Figure 3.3).

3.2 Photosensitivity of 4c

Photosensitivity was measured by UV-Vis spectroscopy. As shown in Figure 4, a series of UV-Vis spectra of **4c** (dissolved in ethyl acetate, room temperature) was collected under the UV irradiation (365 nm, 1 mW/cm^2) for 2 s, 5 s, 10 s, and 30 s. All these spectra exhibited a similar pattern: a strong band and a weak band in the regions of 330 – 340 nm and 430 – 450 nm,

respectively. The strong band is attributed by the π–π* transition of the azo unit, which indicates the presence of *trans* isomer, while the weak band is ascribed to the *cis* n–π* transition in cis isomer.[5] As the UV irradiation time prolonged, the intensity of the strong band decreased rapidly, whereas the signal of the weak band gradually increased. This pattern indicates the occurrence of *trans* → *cis* photoisomerisation.[5] Interestingly, dissolved **4c** reached photostationary state in 10 seconds, significantly faster than reported response rates of similar ABLCs, which are in minutes and even hours.[11,13,14,16–18,22,24,49–52]

Compound **4c** can turn from crystalline solid into nematic phase (Figure S2.1) by heating the pure sample to 95 °C. Under the UV irradiation (365 nm, 1 nW/cm^2), nematic **4c** became isotropic liquid in 3 seconds (Figure S2.2). Without the UV irradiation, **4c** restored to nematic phase within 5 seconds under indoor natural visible light (Figure S2.1). These phenomena indicate the presence of reversible *trans – cis* photoisomerisation. The UV-induced *cis* isomers destabilised the orderly arrangement of *trans* isomers in nematic phase and possibly reduced the phase transition temperatures.[1,24] Under visible light, the backward *trans* ← *cis* photoisomerisation started and restored the nematic phase of ***4c***.

The ratio of the isomer concentrations can be estimated by the following equation:

$$[cis]_t / [trans]_0 = (1 - A_t / A_0) / (1 - \varepsilon_{cis} / \varepsilon_{trans})^{53,54}$$

where $[cis]_t$ is the concentration of *cis* isomer at time *t*, $[\text{trans}]_0$ the initial concentration of *trans* isomer, A_0 and A_t are the absorbances at the wavelength of the same chromophore of sample compound, in which all sample compounds in solution are either *trans* or *cis* isomers, ε_{cis} and ε_{trans} the molar attenuation coefficients (also known as molar extinction coefficient and molar absorption coefficient) of the *cis* and *trans* isomers at a given wavelength of light, respectively.[54]

Previous studies on similar azobenzene-based compounds report ε_{cis} / ε_{trans} ratios of 0.050, 0.053, 0.055, 0.056, and 0.05, corresponding to UV wavelengths of 320 nm,[54] 325 nm,[54] 355 nm,[55] 369.5 nm,[56] and 370 nm,[57] respectively. Therefore, we selected 0.05 as the ε_{cis} / ε_{trans} ratio to estimate the isomer fraction under the irradiation of 365 nm UV. The strong absorption band at 334 nm collected from the 30-second UV irradiation test generated a A_t / A_0 ratio of 0.2348, giving a $[cis]_t$ / $[trans]_0$ ratio of 0.81. This ratio indicates that 81% of nematic **4c** had converted from *trans* to *cis* isomers, which is one of the highest among the reported ratios of similar azobenzene-based compounds.[55–61]

3.3 Effect of changing azo position

ABLC compounds are unsuitable for practical applications due to one or more of the following traits: (1) narrow temperature windows of nematic phases, (2) high phase transition temperature, and (3) long period of light stimulation to reach photostationary state.[5] Typical ABLC compounds utilised ester and azo groups as bridging units, in which the azo and ester groups are implemented as side-arms and direct linkages of the central bent core, respectively. We postulated that one major contributor is the strong intermolecular forces of ABLCs and proposed to use two azo bonds as the linkages to the central bent-core in order to reduce the intermolecular interactions. Previous studies suggest that changing the position of azo groups does not improve the mesogenic properties of ABLC.[14,22] However, their investigation focused on the effect of swapping one azo group with ester linkage and did not consider the scenario of linking two azo groups directly to the central bent-core.

To examining our hypothesis, molecular properties of **4c** and its counterpart **4c-c** using two esters as central linkages were calculated and compared as shown in Figure 5. The comparison shows that the dipole moments of *trans* **4c** (3.36 Debye) is significantly smaller than that of **4c-c**

(6.56 Debye). Interestingly, the dipole moment of *cis* **4c** (3.69 Debye) is slightly larger than that of **4c-c** (3.50 Debye). Small dipole moment indicates weak electrostatic interactions, which could promote the low melting point and wide temperature windows of nematic phase of *trans* **4c**. In addition, the molecular structures of **4c** isomers prone to form an orderly geometry likely due to the small molecular structures attaching to the rotatable ester bonds. Therefore, applying azo group as the central linkage to the bent core can lower the melting point and broaden the temperature windows of mesogenic phases.

Moreover, the overall polarisabilities of *trans* and *cis* of **4c** are substantially higher than those of **4c-c**, which corroborates the experimental observations that 4c is superior to its counterpart **4c-c** in terms of *trans* – *cis* photoisomerisation rates. At zero frequency, the isotropic averages of first polarisability of *trans* and *cis* isomers of **4c** (632.7 and 612.5 au^3) are noticeably higher than that of **4c-c** (621.5 and 601.2 au^3), respectively. Interestingly, the average SHG values of **4c** isomers (1900 and 220 au^5) are smaller than those of **4c-c** (2063 and 542 au^5), whereas the third polarisability mean values of **4c** (5.92×10^5 and 2.04×10^5 au) are nearly two times of those of **4c-c** (3.39×10^5 and 1.16×10^5 au). Additional research is necessary to determine the relationship between the molecular properties and bulk performance of this type of material.

4. Conclusion

To date, this is the first study using two azo bonds as direct linkages of the central bent-core to synthesize azobenzene-based bent-core liquid crystal. This compound exhibited a broad temperature window of nematic phase and rapid *trans* – *cis* photoisomerisation in seconds. Quantum mechanics calculations suggest that when two azo bonds instead of esters serve as the linkage on the central bent-core, the electrostatic interactions are substantially weakened and molecular polarisabilities are enhanced. This finding indicates using azo bonds as central linkages

281 can promote favourable phase behaviours and optical properties. In summary, this study proposed
282 a novel method to synthesise photosensitive liquid crystal compound and deployed synergistic
283 approach to mechanistically elucidate material properties. Such efforts are imperative for
284 advancing future design of azobenzene-based bent-core liquid crystals.

285

Acknowledgements

This study was supported by National Natural Science Foundation of China under Grants 11074054 and 11374067. This work used the Extreme Science and Engineering Discovery Environment (XSEDE), which is supported by National Science Foundation grant number ACI-1548562.[62] Specifically, it used the Bridges system, which is supported by NSF award number ACI-1445606, at the Pittsburgh Supercomputing Center (PSC).[63] The computation jobs were submitted through a web-based interface maintained by the Perri Group at Sonoma State University, USA.[64]

Disclosure statement

No potential conflict of interest was reported by the authors.

ORCID

Z. Zhang http://orcid.org/0000-0002-0807-8991

Z. Zhang https://orcid.org/0000-0002-9400-3274

References

(1) Ikeda, T.; Tsutsumi, O. Optical Switching and Image Storage by Means of Azobenzene Liquid-Crystal Films. *Science* **1995**, *268* (5219), 1873–1875. https://doi.org/10.1126/science.268.5219.1873.

(2) Finkelmann, H.; Nishikawa, E.; Pereira, G. G.; Warner, M. A New Opto-Mechanical Effect in Solids. *Phys. Rev. Lett.* **2001**, *87* (1), 015501. https://doi.org/10.1103/PhysRevLett.87.015501.

(3) Reddy, R. A.; Tschierske, C. Bent-Core Liquid Crystals: Polar Order, Superstructural Chirality and Spontaneous Desymmetrisation in Soft Matter Systems. *J. Mater. Chem.* **2006**, *16* (10), 907–961. https://doi.org/10.1039/B504400F.

(4) Mahimwalla, Z.; Yager, K. G.; Mamiya, J.; Shishido, A.; Priimagi, A.; Barrett, C. J. Azobenzene Photomechanics: Prospects and Potential Applications. *Polym. Bull.* **2012**, *69* (8), 967–1006. https://doi.org/10.1007/s00289-012-0792-0.

(5) Alaasar, M. Azobenzene-Containing Bent-Core Liquid Crystals: An Overview. *Liquid Crystals* **2016**, *43* (13–15), 2208–2243. https://doi.org/10.1080/02678292.2016.1175676.

(6) Merino, E.; Ribagorda, M. Control over Molecular Motion Using the *Cis* – *Trans* Photoisomerization of the Azo Group. *Beilstein J. Org. Chem.* **2012**, *8*, 1071–1090. https://doi.org/10.3762/bjoc.8.119.

(7) Natansohn, A.; Rochon, P. Photoinduced Motions in Azo-Containing Polymers. *Chem. Rev.* **2002**, *102* (11), 4139–4176. https://doi.org/10.1021/cr970155y.

(8) Camacho-Lopez, M.; Finkelmann, H.; Palffy-Muhoray, P.; Shelley, M. Fast Liquid-Crystal Elastomer Swims into the Dark. *Nature Mater* **2004**, *3* (5), 307–310. https://doi.org/10.1038/nmat1118.

(9) Wang, Y.; Li, Q. Light-Driven Chiral Molecular Switches or Motors in Liquid Crystals. *Adv. Mater.* **2012**, *24* (15), 1926–1945. https://doi.org/10.1002/adma.201200241.

(10) Garcia-Amorós, J.; Reig, M.; Castro, M. C. R.; Cuadrado, A.; Raposo, M. M. M.; Velasco, D. Molecular Photo-Oscillators Based on Highly Accelerated Heterocyclic Azo Dyes in Nematic Liquid Crystals. *Chem. Commun.* **2014**, *50* (51), 6704–6706. https://doi.org/10.1039/C4CC01450B.

(11) Sunil, B. N.; Srinatha, M. K.; Shanker, G.; Hegde, G.; Alaasar, M.; Tschierske, C. Effective Tuning of Optical Storage Devices Using Photosensitive Bent-Core Liquid Crystals. *Journal of Molecular Liquids* **2020**, *304*, 112719. https://doi.org/10.1016/j.molliq.2020.112719.

(12) Rahman, M. L.; Asik, J.; Kumar, S.; Tschierske, C. Liquid Crystalline Banana-shaped Monomers Derived from 2,7-naphthalene: Synthesis and Properties. *Liquid Crystals* **2008**, *35* (11), 1263–1270. https://doi.org/10.1080/02678290802513808.

(13) Lutfor, M. R.; Hegde, G.; Kumar, S.; Tschierske, C.; Chigrinov, V. G. Synthesis and Characterization of Bent-Shaped Azobenzene Monomers: Guest–Host Effects in Liquid Crystals with Azo Dyes for Optical Image Storage Devices. *Optical Materials* **2009**, *32* (1), 176–183. https://doi.org/10.1016/j.optmat.2009.07.006.

(14) Nagaveni, N. G.; Raghuvanshi, P.; Roy, A.; Prasad, V. Azo-Functionalised Achiral Bent-Core Liquid Crystalline Materials: Effect of Presence of –N=N– Linkage at Different Locations in the Molecular Architecture. *Liquid Crystals* **2013**, *40* (9), 1238–1254. https://doi.org/10.1080/02678292.2013.805831.

(15) Ghosh, S.; Begum, N.; Turlapati, S.; Roy, S. Kr.; Das, Abhijit. Kr.; Rao, N. V. S. Ferroelectric-like Switching in the Nematic Phase of Four-Ring Bent-Core Liquid Crystals. *J. Mater. Chem. C* **2014**, *2* (3), 425–431. https://doi.org/10.1039/C3TC31800A.

(16) Paterson, D. A.; Xiang, J.; Singh, G.; Walker, R.; Agra-Kooijman, D. M.; Martínez-Felipe, A.; Gao, M.; Storey, J. M. D.; Kumar, S.; Lavrentovich, O. D.; Imrie, C. T. Reversible Isothermal Twist–Bend Nematic–Nematic Phase Transition Driven by the Photoisomerization of an Azobenzene-Based Nonsymmetric Liquid Crystal Dimer. *J. Am. Chem. Soc.* **2016**, *138* (16), 5283–5289. https://doi.org/10.1021/jacs.5b13331.

(17) Alaasar, M.; Poppe, S. Cybotactic Nematic Phases with Wide Ranges in Photoresponsive Polycatenars. *Liquid Crystals* **2019**, 1–11. https://doi.org/10.1080/02678292.2019.1690062.

(18) Alaasar, M.; Prehm, M.; Tschierske, C. Influence of Halogen Substituent on the Mesomorphic Properties of Five-Ring Banana-Shaped Molecules with Azobenzene Wings. *Liquid Crystals* **2013**, *40* (5), 656–668.

https://doi.org/10.1080/02678292.2013.767949.
(19) Horčic, M.; Kozmík, V.; Svoboda, J.; Novotná, V.; Pociecha, D. Transformation from a Rod-like to a Hockey-Stick-like and Bent-Shaped Molecule in 3,4′-Disubstituted Azobenzene-Based Mesogens. *J. Mater. Chem. C* **2013**, *1* (45), 7560. https://doi.org/10.1039/c3tc31593b.
(20) Gimeno, N.; Pintre, I.; Martínez-Abadía, M.; Serrano, J. L.; Ros, M. B. Bent-Core Liquid Crystal Phases Promoted by Azo-Containing Molecules: From Monomers to Side-Chain Polymers. *RSC Adv.* **2014**, *4* (38), 19694–19702. https://doi.org/10.1039/C4RA02079K.
(21) Dingemans, T. J.; Murthy, N. S.; Samulski, E. T. Javelin-, Hockey Stick-, and Boomerang-Shaped Liquid Crystals. Structural Variations on *p* -Quinquephenyl †. *J. Phys. Chem. B* **2001**, *105* (37), 8845–8860. https://doi.org/10.1021/jp010869j.
(22) Monika, M.; Prasad, V.; Nagaveni, N. G. Hockey Stick-Shaped Azo Compounds: Effect of Linkage Groups and Their Direction of Linking on Mesomorphic Properties. *Liquid Crystals* **2015**, *42* (10), 1490–1505. https://doi.org/10.1080/02678292.2015.1066889.
(23) Bobrovsky, A.; Shibaev, V.; Hamplová, V.; Bubnov, A.; Novotná, V.; Kašpar, M.; Piryazev, A.; Anokhin, D.; Ivanov, D. Photo-Optical Properties of Amorphous and Crystalline Films of Azobenzene-Containing Photochromes with Bent-Shaped Molecular Structure. *Journal of Photochemistry and Photobiology A: Chemistry* **2016**, *316*, 75–87. https://doi.org/10.1016/j.jphotochem.2015.10.021.
(24) Alaasar, M.; Prehm, M.; Tschierske, C. Helical Nano-Crystallite (HNC) Phases: Chirality Synchronization of Achiral Bent-Core Mesogens in a New Type of Dark Conglomerates. *Chem. Eur. J.* **2016**, *22* (19), 6583–6597. https://doi.org/10.1002/chem.201505016.
(25) Alaasar, M.; Prehm, M.; Brautzsch, M.; Tschierske, C. 4-Methylresorcinol Based Bent-Core Liquid Crystals with Azobenzene Wings – a New Class of Compounds with Dark Conglomerate Phases. *J. Mater. Chem. C* **2014**, *2* (28), 5487–5501. https://doi.org/10.1039/C4TC00533C.
(26) Alaasar, M.; Prehm, M.; May, K.; Eremin, A.; Tschierske, C. 4-Cyanoresorcinol-Based Bent-Core Mesogens with Azobenzene Wings: Emergence of Sterically Stabilized Polar Order in Liquid Crystalline Phases. *Adv. Funct. Mater.* **2014**, *24* (12), 1703–1717. https://doi.org/10.1002/adfm.201302295.
(27) Alaasar, M.; Prehm, M.; Brautzsch, M.; Tschierske, C. Dark Conglomerate Phases of Azobenzene Derived Bent-Core Mesogens – Relationships between the Molecular Structure and Mirror Symmetry Breaking in Soft Matter. *Soft Matter* **2014**, *10* (37), 7285–7296. https://doi.org/10.1039/C4SM01255K.
(28) Yi, W.; Cai, C. Highly Efficient Dinitration of Aromatic Compounds in Fluorous Media Using Ytterbium Perfluorooctanesulfonate and Perfluorooctanesulfonic Acid as Catalysts. *Synthetic Communications* **2006**, *36* (20), 2957–2961. https://doi.org/10.1080/00397910600773700.
(29) Meng, G.; Zheng, M.-L.; Zheng, A.-Q.; Wang, M.; Shi, J. The Novel Usage of Thiourea Nitrate in Aryl Nitration. *Chinese Chemical Letters* **2014**, *25* (1), 87–89. https://doi.org/10.1016/j.cclet.2013.09.003.
(30) Hegde, G.; Rajkumar, Y. A.; Mei, G. S.; Mahmood, S.; Mandal, U. K.; Sudhakar, A. A. Photoisomerization Behavior of Photochromic Amide-Based Azobenzene Dyes Exhibiting H-Bonding Effect: Synthesis and Characterization. *Korean J. Chem. Eng.* **2016**, *33* (4), 1480–1488. https://doi.org/10.1007/s11814-015-0259-8.
(31) Mathews, M.; Kang, S.; Kumar, S.; Li, Q. Designing Bent-Core Nematogens towards Biaxial Nematic Liquid Crystals. *Liquid Crystals* **2011**, *38* (1), 31–40. https://doi.org/10.1080/02678292.2010.524716.
(32) Hanwell, M. D.; Curtis, D. E.; Lonie, D. C.; Vandermeersch, T.; Zurek, E.; Hutchison, G. R. Avogadro: An Advanced Semantic Chemical Editor, Visualization, and Analysis Platform. *J Cheminform* **2012**, *4* (1), 17. https://doi.org/10.1186/1758-2946-4-17.
(33) Wang, J.; Wang, W.; Kollman, P. A.; Case, D. A. Automatic Atom Type and Bond Type Perception in Molecular Mechanical Calculations. *Journal of Molecular Graphics and Modelling* **2006**, *25* (2), 247–260. https://doi.org/10.1016/j.jmgm.2005.12.005.
(34) Wang, J.; Wolf, R. M.; Caldwell, J. W.; Kollman, P. A.; Case, D. A. Development and Testing of a General Amber Force Field. *J. Comput. Chem.* **2004**, *25* (9), 1157–1174. https://doi.org/10.1002/jcc.20035.
(35) *Avogadro: An Open-Source Molecular Builder and Visualization Tool. Version 1.2.0*.
(36) Harada, J.; Ogawa, K.; Tomoda, S. Molecular Motion and Conformational Interconversion of

Azobenzenes in Crystals as Studied by X-Ray Diffraction. *Acta Crystallogr B Struct Sci* **1997**, *53* (4), 662–672. https://doi.org/10.1107/S0108768197002772.

(37) Biswas, N.; Umapathy, S. Density Functional Calculations of Structures, Vibrational Frequencies, and Normal Modes of *Trans* - and *Cis* -Azobenzene. *J. Phys. Chem. A* **1997**, *101* (30), 5555–5566. https://doi.org/10.1021/jp970312x.

(38) Stewart, J. J. P. Optimization of Parameters for Semiempirical Methods VI: More Modifications to the NDDO Approximations and Re-Optimization of Parameters. *J Mol Model* **2013**, *19* (1), 1–32. https://doi.org/10.1007/s00894-012-1667-x.

(39) Baker, J. An Algorithm for the Location of Transition States. *J. Comput. Chem.* **1986**, *7* (4), 385–395. https://doi.org/10.1002/jcc.540070402.

(40) Gordon, M. S.; Schmidt, M. W. Advances in Electronic Structure Theory. In *Theory and Applications of Computational Chemistry*; Elsevier, 2005; pp 1167–1189. https://doi.org/10.1016/B978-044451719-7/50084-6.

(41) Schmidt, M. W.; Baldridge, K. K.; Boatz, J. A.; Elbert, S. T.; Gordon, M. S.; Jensen, J. H.; Koseki, S.; Matsunaga, N.; Nguyen, K. A.; Su, S.; Windus, T. L.; Dupuis, M.; Montgomery, J. A. General Atomic and Molecular Electronic Structure System. *J. Comput. Chem.* **1993**, *14* (11), 1347–1363. https://doi.org/10.1002/jcc.540141112.

(42) Ditchfield, R.; Hehre, W. J.; Pople, J. A. Self-Consistent Molecular-Orbital Methods. IX. An Extended Gaussian-Type Basis for Molecular-Orbital Studies of Organic Molecules. *The Journal of Chemical Physics* **1971**, *54* (2), 724–728. https://doi.org/10.1063/1.1674902.

(43) Hehre, W. J.; Ditchfield, R.; Pople, J. A. Self—Consistent Molecular Orbital Methods. XII. Further Extensions of Gaussian—Type Basis Sets for Use in Molecular Orbital Studies of Organic Molecules. *The Journal of Chemical Physics* **1972**, *56* (5), 2257–2261. https://doi.org/10.1063/1.1677527.

(44) Stephens, P. J.; Devlin, F. J.; Chabalowski, C. F.; Frisch, M. J. Ab Initio Calculation of Vibrational Absorption and Circular Dichroism Spectra Using Density Functional Force Fields. *J. Phys. Chem.* **1994**, *98* (45), 11623–11627. https://doi.org/10.1021/j100096a001.

(45) Becke, A. D. Density-functional Thermochemistry. III. The Role of Exact Exchange. *The Journal of Chemical Physics* **1993**, *98* (7), 5648–5652. https://doi.org/10.1063/1.464913.

(46) O'boyle, N. M.; Tenderholt, A. L.; Langner, K. M. cclib: A Library for Package-Independent Computational Chemistry Algorithms. *J. Comput. Chem.* **2008**, *29* (5), 839–845. https://doi.org/10.1002/jcc.20823.

(47) Kanis, D. R.; Ratner, M. A.; Marks, T. J. Design and Construction of Molecular Assemblies with Large Second-Order Optical Nonlinearities. Quantum Chemical Aspects. *Chem. Rev.* **1994**, *94* (1), 195–242. https://doi.org/10.1021/cr00025a007.

(48) Kurtz, H. A.; Stewart, J. J. P.; Dieter, K. M. Calculation of the Nonlinear Optical Properties of Molecules. *J. Comput. Chem.* **1990**, *11* (1), 82–87. https://doi.org/10.1002/jcc.540110110.

(49) Choi, S.-W.; Izumi, T.; Hoshino, Y.; Takanishi, Y.; Ishikawa, K.; Watanabe, J.; Takezoe, H. Circular-Polarization-Induced Enantiomeric Excess in Liquid Crystals of an Achiral, Bent-Shaped Mesogen. *Angew. Chem. Int. Ed.* **2006**, *45* (9), 1382–1385. https://doi.org/10.1002/anie.200503767.

(50) Vera, F.; Tejedor, R. M.; Romero, P.; Barberá, J.; Ros, M. B.; Serrano, J. L.; Sierra, T. Light-Driven Supramolecular Chirality in Propeller-Like Hydrogen-Bonded Complexes That Show Columnar Mesomorphism. *Angew. Chem. Int. Ed.* **2007**, *46* (11), 1873–1877. https://doi.org/10.1002/anie.200603796.

(51) Mathews, M.; Zola, R. S.; Yang, D.; Li, Q. Thermally, Photochemically and Electrically Switchable Reflection Colors from Self-Organized Chiral Bent-Core Liquid Crystals. *J. Mater. Chem.* **2011**, *21* (7), 2098–2103. https://doi.org/10.1039/C0JM03479G.

(52) Senyuk, B.; Wonderly, H.; Mathews, M.; Li, Q.; Shiyanovskii, S. V.; Lavrentovich, O. D. Surface Alignment, Anchoring Transitions, Optical Properties, and Topological Defects in the Nematic Phase of Thermotropic Bent-Core Liquid Crystal A131. *Phys. Rev. E* **2010**, *82* (4), 041711. https://doi.org/10.1103/PhysRevE.82.041711.

(53) Fischer, E. Calculation of Photostationary States in Systems A .Dblarw. B When Only A Is Known. *J. Phys.*

Chem. **1967**, *71* (11), 3704–3706. https://doi.org/10.1021/j100870a063.
(54) Victor, J. G.; Torkelson, J. M. On Measuring the Distribution of Local Free Volume in Glassy Polymers by Photochromic and Fluorescence Techniques. *Macromolecules* **1987**, *20* (9), 2241–2250. https://doi.org/10.1021/ma00175a032.
(55) Morishima, Y.; Tsuji, M.; Kamachi, M.; Hatada, K. Photochromic Isomerization of Azobenzene Moieties Compartmentalized in Hydrophobic Microdomains in a Microphase Structure of Amphiphilic Polyelectrolytes. *Macromolecules* **1992**, *25* (17), 4406–4410. https://doi.org/10.1021/ma00043a025.
(56) Sasaki, T.; Ikeda, T.; Ichimura, K. Photoisomerization and Thermal Isomerization Behavior of Azobenzene Derivatives in Liquid-Crystalline Polymer Matrixes. *Macromolecules* **1993**, *26* (1), 151–154. https://doi.org/10.1021/ma00053a023.
(57) Wang, W.; Wang, M.-Z. Effect of α-Cyclodextrin on the Photoisomerization of Azobenzene Functionalized Hydroxypropyl Methylcellulose in Aqueous Solution. *Polym. Bull.* **2007**, *59* (4), 537–544. https://doi.org/10.1007/s00289-007-0789-2.
(58) Aronzon, D.; Levy, E. P.; Collings, P. J.; Chanishvili, A.; Chilaya, G.; Petriashvili, G. Trans–Cis Isomerization of an Azoxybenzene Liquid Crystal. *Liquid Crystals* **2007**, *34* (6), 707–718. https://doi.org/10.1080/02678290701267480.
(59) Ya, Q.; Dong, X.-Z.; Chen, W.-Q.; Duan, X.-M. The Synthesis of Aminoazobenzenes and the Effect of Intermolecular Hydrogen Bonding on Their Photoisomerization. *Dyes and Pigments* **2008**, *79* (2), 159–165. https://doi.org/10.1016/j.dyepig.2008.02.004.
(60) Fischer, E. Temperature Dependence of Photoisomerization Equilibria. Part I. Azobenzene and the Azonaphthalenes. *J. Am. Chem. Soc.* **1960**, *82* (13), 3249–3252. https://doi.org/10.1021/ja01498a005.
(61) Naito, T.; Horie, K.; Mita, I. Photochemistry in Polymer Solids. 11. The Effects of the Size of Reaction Groups and the Mode of Photoisomerization on Photochromic Reactions in Polycarbonate Film. *Macromolecules* **1991**, *24* (10), 2907–2911. https://doi.org/10.1021/ma00010a042.
(62) Towns, J.; Cockerill, T.; Dahan, M.; Foster, I.; Gaither, K.; Grimshaw, A.; Hazlewood, V.; Lathrop, S.; Lifka, D.; Peterson, G. D.; Roskies, R.; Scott, J. R.; Wilkins-Diehr, N. XSEDE: Accelerating Scientific Discovery. *Comput. Sci. Eng.* **2014**, *16* (5), 62–74. https://doi.org/10.1109/MCSE.2014.80.
(63) Nystrom, N. A.; Levine, M. J.; Roskies, R. Z.; Scott, J. R. Bridges: A Uniquely Flexible HPC Resource for New Communities and Data Analytics. In *Proceedings of the 2015 XSEDE Conference on Scientific Advancements Enabled by Enhanced Cyberinfrastructure - XSEDE '15*; ACM Press: St. Louis, Missouri, 2015; pp 1–8. https://doi.org/10.1145/2792745.2792775.
(64) Perri, M. J.; Weber, S. H. Web-Based Job Submission Interface for the GAMESS Computational Chemistry Program. *J. Chem. Educ.* **2014**, *91* (12), 2206–2208. https://doi.org/10.1021/ed5004228.

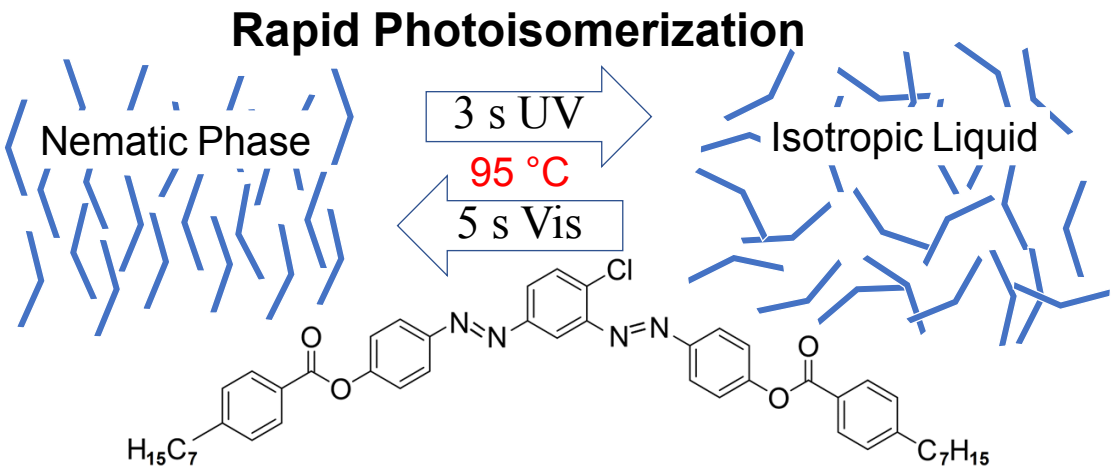

Graphical Abstract

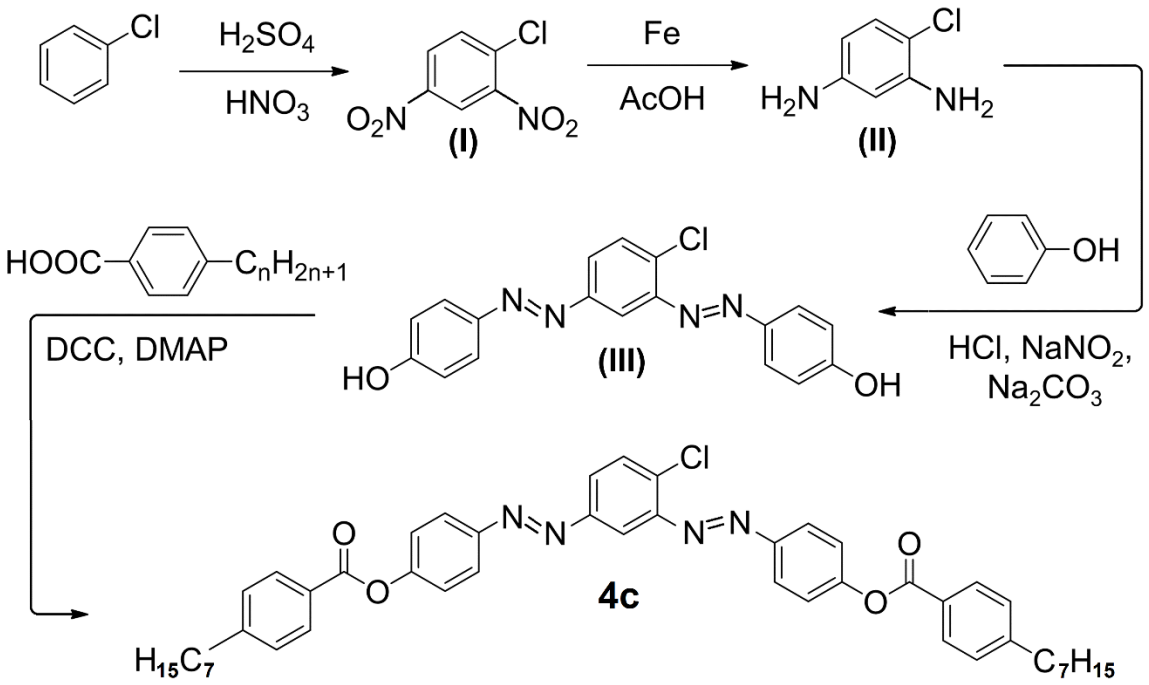

Figure 1. Synthesis of 4-chloro-1,3-diazobenzene bent-core liquid crystal.

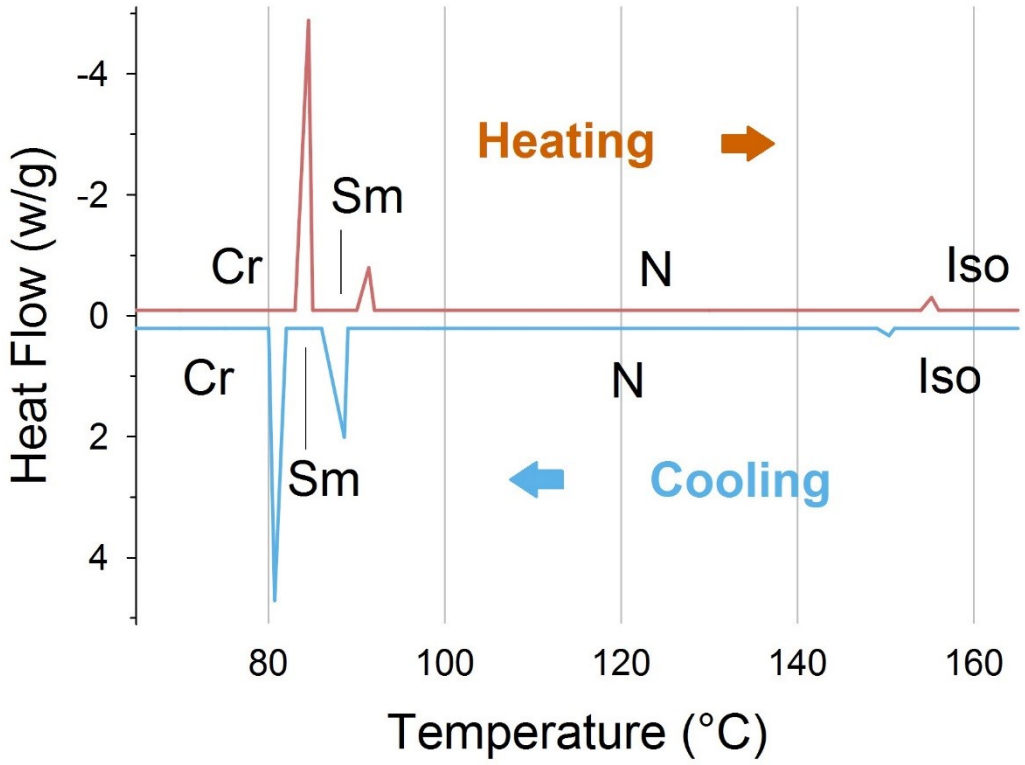

Figure 2. DSC heating and cooling traces of compound **4c**.

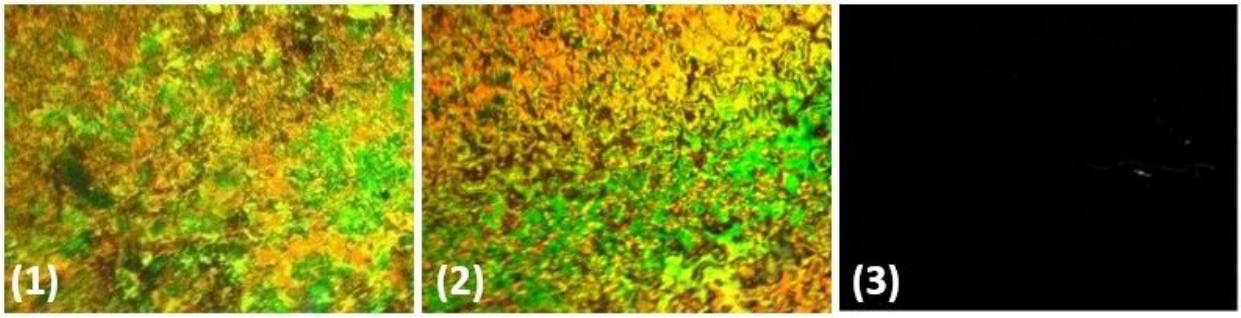

Figure 3. Polarised optical micrograms of compound **4c** under various conditions: (1) smectic textures at 88 °C, (2) nematic textures at 120 °C, and (3) isotropic liquid phase at 155 °C.

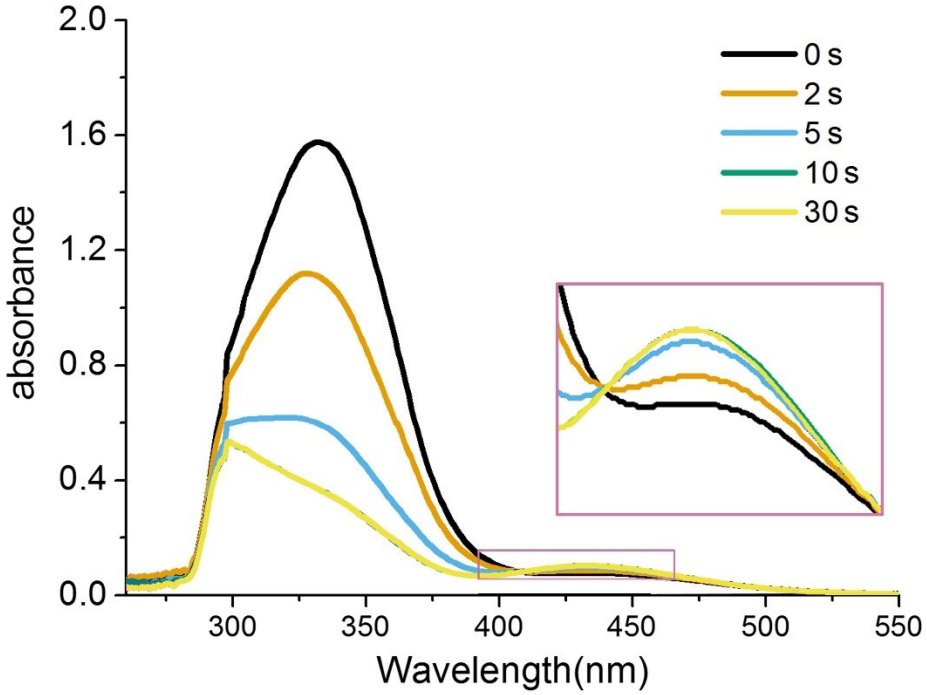

493

494 Figure 4. UV-Vis spectra of dissolved compound **4c** under 365 nm UV irradiation for 0 s, 2 s, 5 s,
495 10 s, and 30 s.

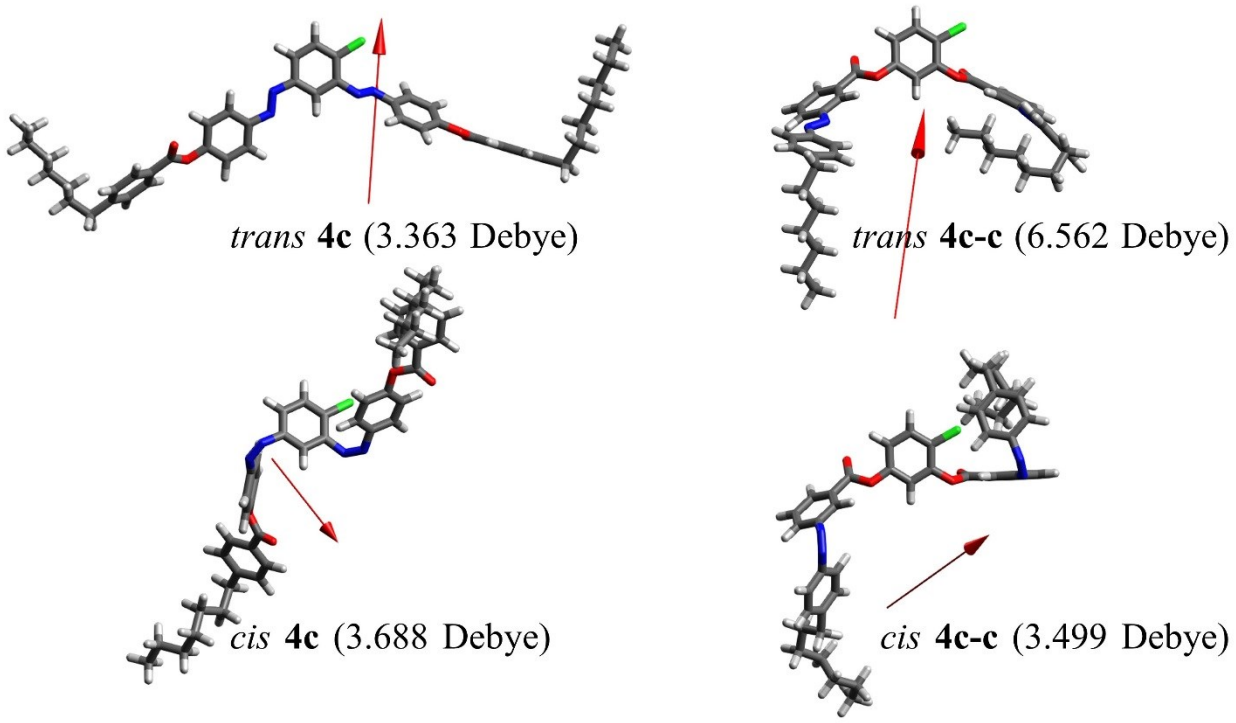

496

497 Figure 5. Molecular structures and dipole moments of isomers of compound **4c** and its

498 counterpart **4c-c** at the ground states. Red arrows represent the direction of dipole moment.